Springer

KSME

Journal of Mechanical Science and Technology 29 (4) (2015) 1689~1696
www.springerlink.com/content/1738-494x
DOI 10.1007/s12206-015-0341-5

Numerical simulation of shock wave and contact surface propagation in micro shock tubes †

Guang Zhang and Heuy Dong Kim*

Department of Mechanical Engineering, Andong National University, Andong, 760-749, Korea

(Manuscript Received July 12, 2014; Revised December 18, 2014; Accepted December 29, 2014)

Abstract

Micro shock tubes have been widely used in many engineering and industrial applications, but their performance and detailed flow characteristics are not well known. Compared to macro shock tubes, unsteady flows related to the moving shock waves in micro shock tubes are highly complicated due to more active viscous dissipation and rarefaction effects. This makes shock wave dynamics significantly different from theoretical predictions. One of the major flow behaviors related to the shock wave propagation in micro shock tube is that the boundary layer growth leads to stronger dissipative shock wave. Due to effects of the scale, more shock wave attenuation happens in micro shock tubes. We used a CFD approach to understand the flow characteristics in a micro shock tube with finite diameter. A fully implicit finite volume scheme has been employed to solve the unsteady compressible Navier-Stokes equations. The diaphragm pressure ratio and diameter of the shock tube were varied to investigate their effects on micro shock tube flows. Based on the predicted results, some wave diagrams were built to characterize the micro shock tube flows. Detailed flow structures between the contact surface and moving shock wave were analyzed during the present study.

Keywords: Shock wave motion; Shock wave attenuation; Contact surface propagation; Unsteady flow; CFD

1. Introduction

Due to their simple structure and micro scale, micro shock tubes have been widely used in various engineering applications, such as micro turbines, micro combustions, and needle-free delivery systems. Micro shock tubes, being similar to conventional shock tubes of larger scale, consist of the driver section and driven section, which are separated by a suitable diaphragm. Due to the pressure difference between the driver section at a high pressure and the driven section at a relatively low pressure, sudden rupture of the diaphragm leads to unsteady flow with shock waves in the shock tube. The shock wave and contact surface move towards the driven section and the expansion head moves into the driver section. Compressible flows with moving shock waves demand further consideration of dissipative effects which are usually absent in macro shock tube flows. Although shock waves have been extensively studied over the last century, there are still some remaining unexplored and unexplained effects on shock wave propagation in micro shock tubes.

The contact surface is an imagined surface of separation between the driver gas and shock heated gas. The temperature of the flow in the front of contact surface is much higher than that behind the contact surface, but pressure and velocity of the flow are same in these two regions. The contact surface is accelerated in the region between the shock wave and contact surface due to boundary layer formation. However, the measurement of its discontinuity is not easy.

Viscous and rarefaction effects caused by low driven pressure and micro scales become more prominent in micro shock tubes. Compared to macro shock tubes, these mentioned effects make micro shock tubes show different shock wave dynamic behavior. One of the major changes related to the decay of shock wave propagation is that the boundary layer growth makes the shock wave more attenuated. Heat conduction phenomena, commonly ignored in conventional shock tubes, play an important role in the micro scale shock tubes, and viscous stresses attenuate both velocity of the flow and shock wave propagation, which makes experimental study difficult to perform compared to numerical analysis. Flow characteristics have been studied by theoretical analysis, numerical simulations and experiments by a great number of researchers in different micro shock tubes.

The viscous loss associated with the boundary layer growth attenuates the shock wave propagation, which was observed by Duff [1]. An electron beam densitometer was used for observing shock velocity attenuation in a low pressure shock

*Corresponding author. Tel.: +82 10 6846 2278, Fax.: +82 54 823 5459
E-mail address: kimhd@andong.ac.kr
† Recommended by Associate Editor Hyoung-gwon Choi

tube. The initial pressure ratio was also observed to influence the shock strength. Zeitoun et al. [2, 3] studied the application of unsteady Navier-Stokes equations coupled with the velocity slip and temperature jump boundary conditions to micro shock tube flows. Knudsen number as an important parameter to investigate micro flow was calculated for simulated cases. Results showed that the unsteady Navier-Stokes equations modeling the micro flow with no-slip wall boundary conditions were valid if Kn was less than 0.01. A strong decrease in the shock strength and the flow velocity along the micro shock tube was observed. The decay of shock wave strength was stronger at lower initial pressure and smaller tube diameter.

Brouillette [4] investigated unsteady micro-scale compressible flows experimentally. He introduced a control volume model and proposed a scaling parameter S which consists of the Reynolds number Re in the region between the shock wave and contact surface multiplied by the shock tube diameter D and divided by the distance 4 L as is shown in Eq. (1). L is the distance between the shock wave and contact surface. Diffusive effects of the friction and heat conduction were studied at low S values in micro shock tubes of low Reynolds number. Results showed that the model predicted the shock wave at small scale to experience much loss in strength and the minimum shock wave velocity determined by viscous effects could become subsonic. In addition, experimental results had quantitative agreement with the theoretical conclusion from the proposed model at low driven pressures in shock tubes.

$$S = \frac{\mathrm{Re}\times D}{4L}. \tag{1}$$

Mirels [5] introduced an analytical method to evaluate boundary layer influence on shock wave propagation. It was assumed that the shock wave moves with uniform velocity, and the flow was investigated in a shock fixed coordinate system. Taking the deviation of free stream conditions between the shock wave and contact surface into account, the parameter β proposed by Roshko, appeared to agree with experimental data to within about 10 percent for shock Mach numbers greater than 5. The basic theory also had agreement with the previous results from Roshko's work.

Sturtevant [6] and Tanaki et al. [7] investigated the influence of boundary layer on the shock wave propagation at different boundary conditions. Good agreement was observed between simulations and theoretical results for the laminar portion of the boundary layer. Ngomo et al. [8] studied the wall friction and heat transfer effects on the shock wave propagation in a micro shock tube. They found that diffusive shear stresses and energy losses near the wall significantly led to shock wave attenuation. Sun et al. [9] performed numerical and experimental studies on shock wave propagation in narrow channels with height ranging from 1 mm to 16 mm. The channel flow was visualized by using double exposure holographic interferometery technique, and pressure transducers were used for recording pressure changes at different locations. Experimental results had a good agreement with numerical results.

Hu et al. [10] did an experimental study on the shock wave attenuation compared to the theoretical results. A decrease in shock wave velocity was observed at different low Reynolds numbers. Results showed that the viscosity of the flow dominated the shock wave attenuation as the shock wave propagated in the overlong channel. Bhasakaran [11] used chemical kinetics and high temperature gas flow to study flows in shock tubes. Based on the Knudsen number, which indicates the rarefaction effects, K. R. Arun and H. D. Kim [12, 13] performed computational studies to investigate the shock wave propagation under different pressure ratios, shock tube diameters and wall boundary conditions. The results indicated shock wave propagation is attenuated by viscous boundary layer formation, and the decay of the shock wave increases drastically with reduction in diameter. Park et al. [14] investigated shock wave propagation and shock wave attenuation. Results indicated shock wave attenuation happened much more in the micro shock tube of smaller scale.

This paper mainly focuses on observing shock wave propagation, contact surface propagation and on giving an indepth analysis for shock wave attenuation at different boundary conditions. Numerical investigations on shock wave and contact surface propagation were carried out in different micro shock tube models. Effects of different diaphragm pressure ratios were investigated by keeping constant pressure in the driven section. Influences of the shock tube diameter on shock wave propagation, shock wave attenuation and boundary layer development were also studied. The contact surface propagation was investigated by obtaining velocity profiles and locations of the contact surface. The distance L between the shock wave and contact surface was obtained for determining the scaling parameter S, which indicates effects of the scale. CFD results were compared with theoretical conclusions and experimental results.

2. Theoretical analysis

2.1 Shock tube theory

After a diaphragm is ruptured, the shock wave and contact surface move into the driven section with Mach number M_S and M_C, while the expansion wave moves towards the driver section. From inviscid theory, the flow viscosity is not taken into account. In the ideal shock tube, the working gas is assumed to be perfect gas with a constant γ and an initially constant temperature. Based on the initial diaphragm pressure ratio P_4/P_1, shock Mach number M_S, contact surface Mach number M_C, expansion head velocity U_{EH} and expansion tail Mach number M_{ET} can be calculated as:

$$\frac{P_4}{P_1} = \left\{1 + \frac{2\gamma_1}{\gamma_1 + 1}\left(M_S^2 - 1\right)\right\} \cdot \left\{1 - \frac{\gamma_4 - 1}{\gamma_4 + 1}\frac{a_1}{a_4}\left(M_S - \frac{1}{M_S}\right)\right\}^{-2\gamma_4/\gamma_4 - 1} \tag{2}$$

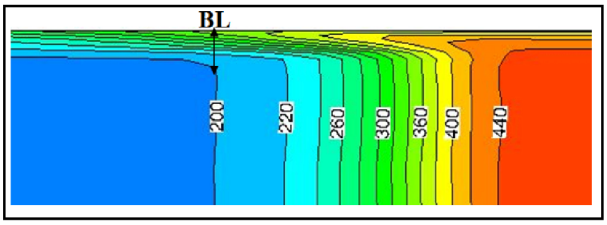

Fig. 1. Temperature contours at t = 0.03 ms (D = 6 mm, Pr = 15).

$$M_C = \frac{1}{\gamma_1}\left(\frac{P_2}{P_1}-1\right)\sqrt{\frac{2\gamma_1}{\gamma_1+1}\frac{\frac{P_2}{P_1}+\frac{\gamma_1-1}{\gamma_1+1}}{\frac{\gamma_1+1}{\gamma_1-1}\frac{P_2}{P_1}+\left(\frac{P_2}{P_1}\right)^2}}\sqrt{\frac{1+\frac{\gamma_1+1}{\gamma_1-1}\frac{P_2}{P_1}}{\frac{\gamma_1+1}{\gamma_1-1}\frac{P_2}{P_1}+\left(\frac{P_2}{P_1}\right)^2}}, \tag{3}$$

$$U_{EH} = -a_4, \tag{4}$$

$$M_{ET} = \frac{2}{\gamma_4-1}\left[1-\left(\frac{P_1}{P_4}\frac{P_2}{P_1}\right)^{\gamma_4-1/2\gamma_4}\right]-\left(\frac{P_1}{P_4}\frac{P_2}{P_1}\right)^{\gamma_4-1/2\gamma_4}. \tag{5}$$

These equations indicate that shock wave and contact surface Mach number, expansion head velocity and expansion tail Mach number remain constant in the micro shock tube as all conditions are fixed. As the diaphragm pressure ratio increases, M_S, M_C and M_{ET} will also increase, but U_{EH} will stay constant. However, due to the attenuation in the real shock tube flow resulting from viscous and rarefaction effects, shock wave and contact surface Mach number will differ from the theoretical solutions from inviscid shock tube theory. Shock wave Mach number will gradually decrease, but contact surface velocity will gradually increase. The expansion head velocity and expansion tail Mach number will also decrease. The formation and development of the boundary layer behind the shock wave is the main reason for this.

Reynolds number was calculated with 6.2×10^4, so a turbulent boundary layer happened in present shock flows. In addition, this also resulted in full turbulent flow in both driver and driven sections. The turbulent boundary layer leads to a larger momentum and energy losses of the flow than the laminar boundary layer as well as more rapid decay of shock wave strength. The boundary layer can be obviously seen in the Fig. 1.

2.2 Scaling parameter S

The momentum conservation related to effects of the micro scale or low Reynolds numbers can be expressed with Navier-Stokes equations from Ref. [15].

$$\rho\frac{D\vec{u}}{Dt}+\nabla P = \mu\nabla^2\vec{u}+\left(\mu_v+\frac{1}{3}\mu\right)\nabla\left(\nabla\vec{u}\right). \tag{6}$$

To simplify Eq. (6), the x direction component of the momentum equation for axisymmetric flow is given as:

$$\rho\frac{\partial u}{\partial t}+\rho u\frac{\partial u}{\partial x}+\frac{\partial P}{\partial x} = \mu\left(\frac{\partial^2 u}{\partial x^2}+\frac{\partial^2 u}{\partial r^2}+\frac{1}{r}\frac{\partial u}{\partial r}\right) + \left(\mu_v+\frac{1}{3}\mu\right)\times\frac{\partial}{\partial x}\left(\frac{\partial u}{\partial x}+\frac{\partial v}{\partial r}+\frac{v}{r}\right), \tag{7}$$

where u = u(x, r) represents the axial velocity of the gas and v is the radial velocity of the gas in micro shock tubes. Assuming that the radial velocity of the gas is zero, incorporating the mass conservation and averaging the velocity Laplacian in the radial direction leads to the following equation.

$$\frac{\partial(\rho u)}{\partial t}+\frac{\partial}{\partial x}\left(\rho u^2+P\right) = C_2\mu\frac{u}{D_h^2} + \left(\mu_v+2\mu\right)\frac{\partial^2 u}{\partial x^2}-\frac{\rho_{h1}}{D_h}\frac{d\delta}{dt}u, \tag{8}$$

where C_2 is a constant used to parameterize the radial velocity gradient in terms of the bulk velocity of fluid inside the shock tube and the diameter of the shock tube. The comparison between this new momentum source in one-dimensional formulation which is derived by averaging the gradient of velocity in the shock tube and the convective momentum transfer is obtained as:

$$G = \frac{\mu\frac{u}{D_h}}{\frac{\partial\rho u}{\partial t}} = \frac{\mu u}{D_h^2}\frac{L/a}{\rho u} = \frac{L}{D_h}\frac{1}{\mathrm{Re}}. \tag{9}$$

This clearly shows that the G value is related to the distance L between the shock wave and contact surface, the tube diameter D_h and the Reynolds number in the region between the shock wave and contact surface. Brouillette [4] introduced a term that is related to G. the term was expressed as S = Re*D/4L = 1/4G, which indicates effects of the scale on shock wave propagation.

Diffusive transport phenomena, such as the heat conduction and shear stresses, lead to remarkable deviation in flow characteristics compared to ideal shock wave behaviors in a micro shock tube as demonstrated by Brouillette. A control volume encompassing the region between the shock wave and the contact surface was proposed to quantify effects of the scale and diffusive transport phenomena on shock wave propagation as is shown in Fig. 2. SW, CS and EW, respectively, represent shock wave, contact surface and expansion waves. Due to diffusive transport effects, there could be a resistance force acting on the control volume, the influence of viscous stresses on shock tube walls, and heat conduction to the walls. With this control volume approach, the friction and heat transfer to side walls are described by appropriate source terms. As the shock wave and contact surface propagate in the driven section, the control volume becomes larger and larger due to

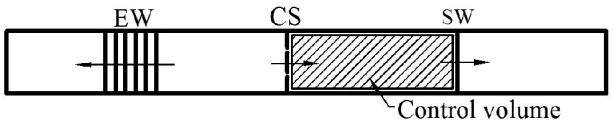

Fig. 2. Control volume used in the study of diffusive effects in the micro shock tube.

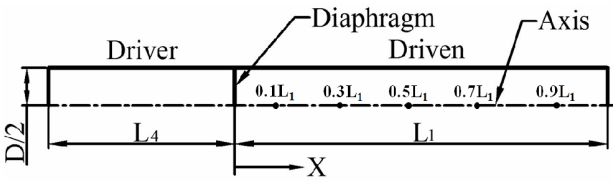

Fig. 3. Schematic of computational domain.

large velocity difference between the shock velocity and contact surface velocity.

Based on the control volume model, the scaling parameter S = Re*D/4L which indicates effects of the scale was used in Eq. (10).

$$\frac{P_2}{P_1}=\frac{\rho_2}{\rho_1}\left\{1+\frac{\gamma_1-1}{2}M_S^2\left[1-\left(\frac{\rho_1}{\rho_2}\right)^2\right]\right\} -\frac{\rho_2}{\rho_1}\left(\frac{4L}{D\,\mathrm{Re}}\right)\frac{1}{M_S\,\mathrm{Pr}}\left[\frac{P_2}{P_1}\frac{\rho_1}{\rho_2}-1\right]. \tag{10}$$

The S value is a noticeable parameter to indicate effects of the scale. Reynolds number and the distance between the shock wave and contact surface should be obtained to calculate S. Note that $Re = u_2\rho_2 D/\mu_2$. The Reynolds number depends on the velocity of the gas, density of the gas and dynamic viscosity in the region between the shock wave and contact surface. Indeed, effects of the scale are affected by Reynolds number and the length L of the control volume. Effects of the scale increase with the decrease of Reynolds number and the increase of the distance between the shock wave and contact surface. As the shock wave and contact surface move in the micro shock tube, these parameters always change. This equation indicates that a smaller S value will have more obvious effects on calculating density ratio between the front and after of shock wave. Small Reynolds number and larger distance L will contribute to smaller S values. If S becomes infinite, effects of the scale can be ignored. This happens in shock tubes with large diameters and high Reynolds numbers.

2.3 Shock wave attenuation

Much more attenuation happens in micro shock tubes compared to macro shock tubes, so it is meaningful to study the decay of shock wave with quantitative methods in micro shock tubes. This can provide an easy way to understand the shock wave propagation. Based on the previous studies, under turbulent flow conditions, the shock wave attenuation $\Delta P_s/\Delta P_{s,i}$ is given by the following equation proposed by Xiao Hu [10].

$$\frac{\Delta P_s}{\Delta P_{s,i}}=1-\frac{\dfrac{0.115}{2(\gamma+1)^{0.2}}}{\left(\dfrac{U_s}{u_2}\right)^{1.4}\left(\dfrac{Da_2}{\upsilon_2}\right)^{0.2}}\left(\frac{x}{D}\right)^{0.8}, \tag{11}$$

where ΔP_s is the shock strength of each testing point and

$\Delta P_{s,i}$ is original point's shock strength (x/D = 0). As the shock wave propagates in the micro shock tube, more and more decay of the shock wave happens due to the friction between the shock wave front and shock tube walls. In addition, boundary layer formation behind the shock wave also contributes to the shock wave attenuation.

3. Computational study

3.1 Computational domain

Unsteady flows were simulated at different initial conditions in micro shock tube models. The driver section and driven section were filled with an ideal gas. For the present study, a 2D axisymmetric micro shock tube model was numerically simulated (Fig. 3). All sections are circular in cross-section with the same diameter. The driver section L_4 is 50 mm long and the driven section L_1 has a length of 100 mm. Five points mounted at the axis of the simulated shock tube model are used for recording pressure changes as shock wave moves through these locations.

3.2 Numerical schemes

To observe the detailed characteristics of unsteady flow, fine structured quad grids were created with boundary layers near walls in all simulation regions. Fine boundary layer grids are required to exactly analyze boundary layer effects on shock wave attenuation. The driver section and the driven section were filled with air assumed as ideal gas., The Knudsen number was calculated with $Kn = 4.12 \times 10^{-5}$, so the flow properties were mathematically analyzed by using unsteady Reynolds Averaged Navier-Stokes equations. The Reynolds number approximated 6.2×10^4 in the present micro shock tube, so the turbulence model was solved by SST k-ω model. Sutherland viscosity model showing variable viscosity with temperature change was used as viscosity model. AUSM scheme was used as the flux model and the second order implicit scheme was used for temporal discretization. Spatial discretization was described by using second order upwind scheme. The driver and driven sections were patched with corresponding initial pressures.

3.3 Boundary conditions

Effects of the diaphragm pressure ratio and shock tube di-

Table 1. Detailed parameters for different CFD cases.

Cases	P_4 (atm)	P_4/P_1	$T_{1,4}$ (K)	Diameters (mm)
1	15	15	300	6
2	30	30	300	6
3	15	15	300	3

ameter were studied at different initial pressures in driver section and different shock tube diameters. Both sections were initialized with the constant total temperature of 300 K. The detailed conditions are given in Table 1.

Commercial solver, Fluent, was used for the simulation of the present micro shock tube models. The mesh size for the simulated model was 156,000 and the minimum cell led to an iteration time step size of 10^{-8} s. The driver section was filled with high pressure ideal gas of 15 atm or 30 atm, and atmospheric pressure was specified in the driven section.

The diaphragm boundary condition was instantaneously removed, which was regarded as the diaphragm being suddenly ruptured. Before the diaphragm was ruptured, in order to check the initializations and boundary conditions, the simulation was performed in some time. After this, the diaphragm was suddenly ruptured. Wall boundary conditions were no-slip and adiabatic walls. For the no-slip wall, the velocity of the flow adhered to the wall was zero (u = 0, v = 0). The axial velocity of the flow increases from zero near the wall to full velocity at the axis in radial direction. The wall temperature was kept a constant of 300 K, so no heat transfer happened between shock heated gas and tube walls.

3.4 Validation

To validate the accuracy of the numerical methods used in the present study, experimental results and CFD results were compared. The experimental data was taken from Ref. [14] where a shock tube of 6 mm diameter was studied at diaphragm pressure ratio of 6. The driver section was initialized at the pressure of 6 atm, and the driven section was kept at atmosphere pressure. Shock wave and expansion wave propagation curves were obtained as is shown in Fig. 4. SW and EH, respectively, represent shock wave and expansion head. The shock wave moved towards the driven section, and the expansion head moved towards the opposite direction. Results show that acceptable deviations were observed except that more attenuation happened in the experimental study due to much more viscous effects in real gas. High viscous effects caused by high temperature happened due to the shock wave heating the real gas behind the shock. In addition, the heat transfer between shock heated gas and tube walls also resulted in much attenuation in the experimental study. For CFD study, the walls were assumed to be adiabatic walls with constant temperature of 300 K. Therefore, simulation schemes used for the present study can predict flow characteristics in micro shock tubes.

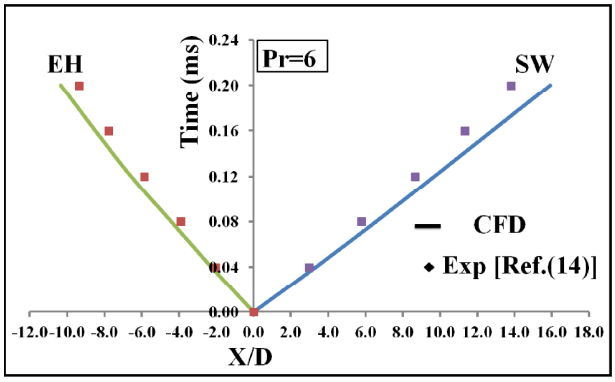

Fig. 4. Comparison between experimental and CFD waves locations at various time (D = 6 mm).

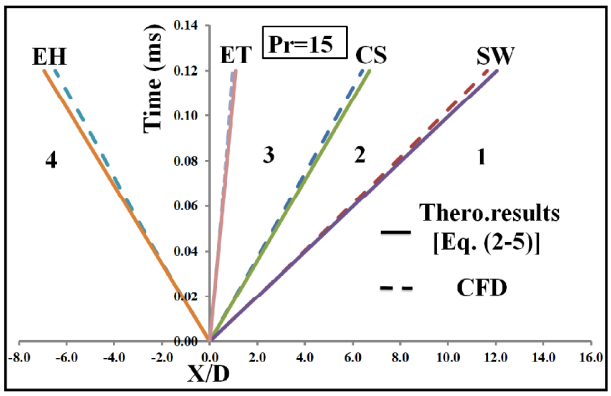

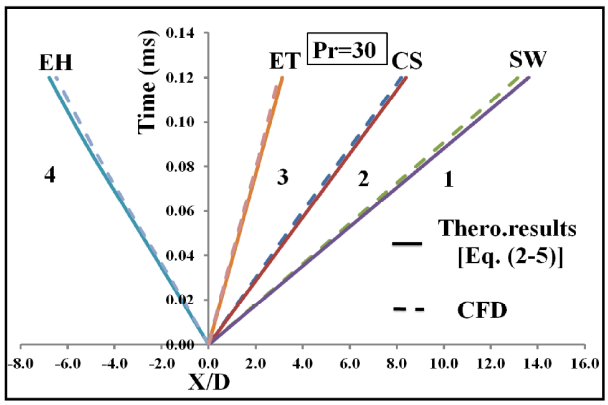

Fig. 5. Shock wave, contact surface and expansion waves locations at various time (D = 6 mm).

4. Results and discussion

Different initial driver pressures were used to study the propagation of waves as is shown in Table 1. As expansion waves did not reach the end wall in the driver section, locations of shock wave, contact surface and expansion waves were obtained as an x-t waves diagram in Fig. 5. SW represents the shock wave, and CS is contact surface. ET represents expansion tail, and EH is expansion head.

Compared to theoretical results calculated from inviscid

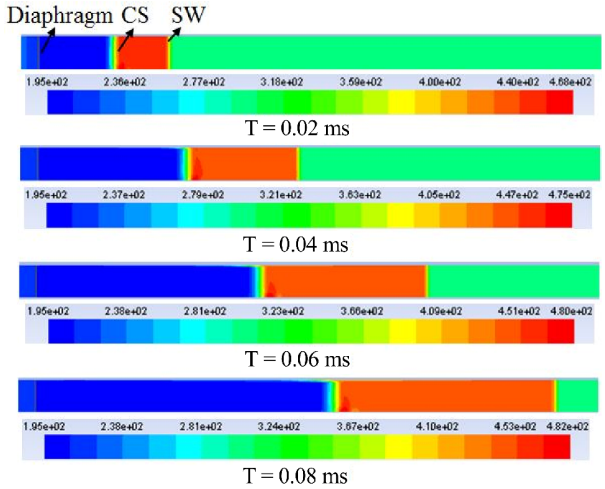

Fig. 6. Temperature contours at various time.

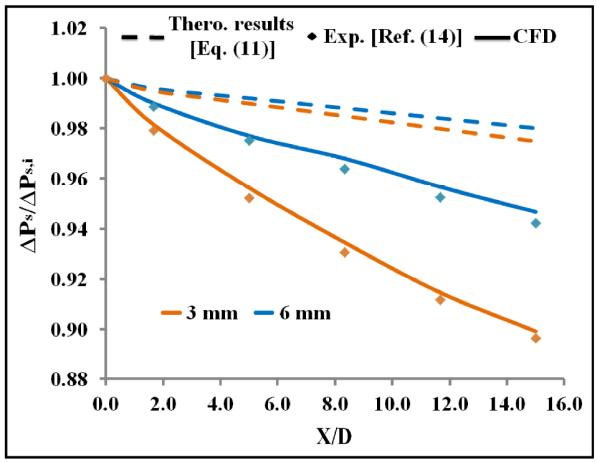

Fig. 7. Shock attenuation distributions for different cases.

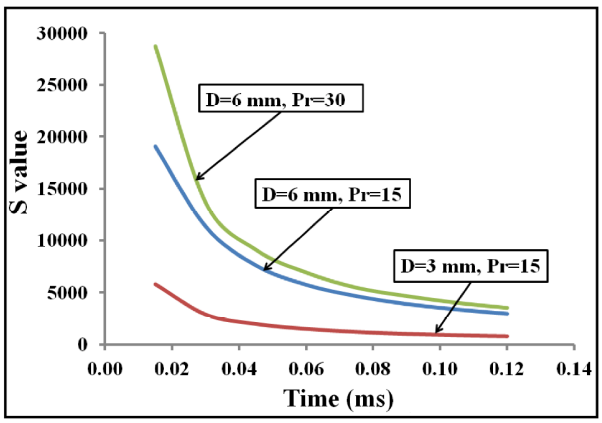

Fig. 8. S value distributions for different cases.

shock tube theory, reasonable deviations show that viscous effects attenuate shock wave, contact surface and expansion wave propagation in CFD simulations. Shock wave and contact surface at pressure ratio of 30 propagated much faster than that at pressure ratio of 15. This indicates that initial diaphragm pressure ratio influences shock wave strength and contact surface propagation. As the diaphragm pressure ratio increases, shock wave and contact surface Mach number also increase, which shows a good agreement with theoretical results calculated from Eqs. (2) and (3). In addition, the expansion tail velocity increases as well. The expected attenuation in wave propagation is obtained in this simulation, which results from viscous effects, the friction between shock wave front and tube walls, and the boundary layer formation behind the shock wave. T = 0.02 ms T = 0.04 ms T = 0.06 ms T = 0.08 ms

The locations of shock wave and contact surface from the diaphragm can be easily seen from the temperature contours, as is shown in Fig. 6. The shock wave moved faster than the contact surface. This led to the distance between shock wave and contact surface becoming larger and larger. The distances were obtained to calculate S values at different time in the micro shock tube.

The shock wave attenuation from experimental and CFD results are compared with theoretical results calculated from Eq. (11) as is shown in Fig. 7. Five fixed points along the axis were used for recording pressure changes in CFD simulations as the shock wave moved through the driven section.

As the shock wave propagated through the driven section, shock wave attenuation gradually increased. The main reasons are that a turbulent boundary layer, where the momentum and energy of the flow inside the boundary layer decrease, developed behind the shock wave and friction occurred between the shock front and tube walls. This made the shock wave lost strength. The deviation between experiment results and theoretical calculations is more obvious, which indicates much more viscous effects exist in the real gas. Much more decay is observed in the shock tube with 3 mm diameter, compared to that in the 6 mm diameter shock tube. This demonstrates that effects of the scale have obvious influence on shock wave propagation in shock tubes of micro scale.

The distributions of scaling parameter S calculated at different diaphragm pressure ratios and shock tube diameters are shown in Fig. 8. As the shock wave moved in micro shock tube, the S value decreased because the distance L used in the scaling parameter S between the shock wave and the contact surface became larger. Relatively high S values in three cases, as is shown in Fig. 8, can be attributed to the reason that high Reynolds numbers were calculated from present cases. S values at the shock tube diameter of 6 mm are much higher than at the shock tube diameter of 3 mm due to higher Reynolds numbers caused by the larger diameter. S values are higher at pressure ratio of 30 compared to that at pressure ratio of 15 in the shock tube of same diameter, which results from higher Reynolds numbers caused by higher flow velocity in the region between shock wave and contact surface at higher diaphragm pressure ratio.

A smaller S value, indicating that effects of the scale are more obvious on shock wave propagation, demonstrates that

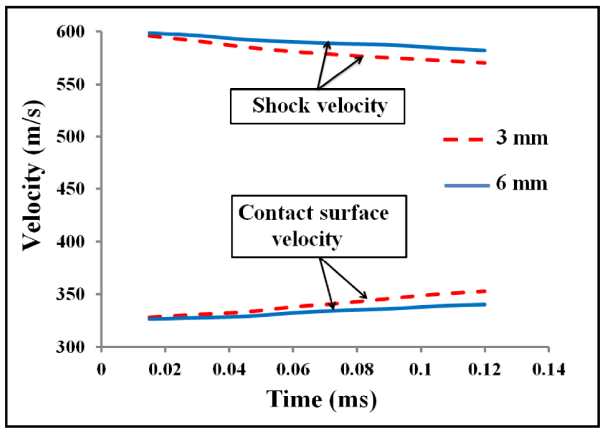

Fig. 9. Velocity distributions of shock wave and contact surface for different tube diameters.

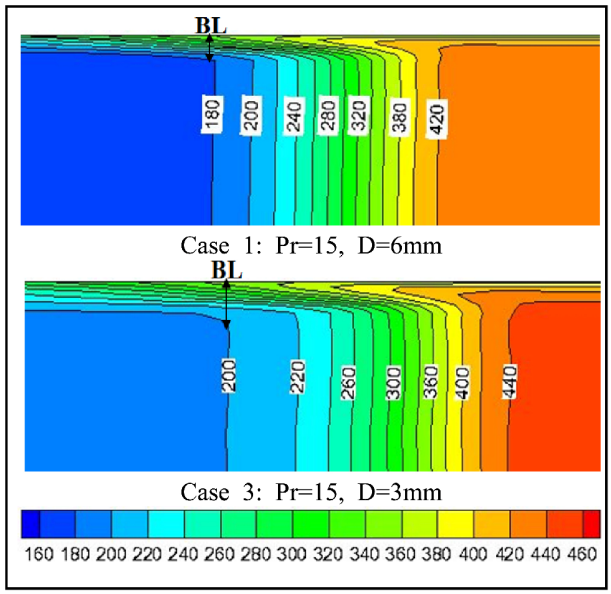

Fig. 10. Temperature distributions for different cases at t = 0.03 ms.

much more attenuation happened in shock tubes of micro scale. From the theoretical Eq. (10), it is well known that as S value decreases, the effect of S value on calculating density ratios becomes more prominent. This shows high S value is not suitable to show effects of the scale on shock wave propagation. A smaller tube diameter and lower pressure in the driven section can lead to smaller S values that show expected effects of the scale.

The shock wave and contact surface velocity distributions are clearly shown in Fig. 9. The distance L between the shock wave and contact surface used to calculate the scaling parameter S can be obtained. The shock wave velocity gradually decreased in both cases due to effects of the friction between the shock front and tube walls and the boundary layer developing behind the shock wave. The contact surface velocity gradually increased due to the boundary layer formation. Boundary layers near tube walls form behind the shock wave, which makes the contact surface propagation similar to that the contact surface moves through a virtual converging-diverging nozzle that accelerates the contact surface. As the contact surface velocity increased, the Reynolds number in the region between the shock wave and contact surface increased, and the distance L between the shock wave and contact surface also increased. This resulted in the decrease of S values due to the increase rate of L being faster than that of Reynolds number.

Shock wave velocity decreased faster, but contact surface velocity increased faster in the shock tube with smaller diameter. This is because a thicker boundary layer developed behind the shock wave in the smaller diameter shock tube.

Temperature contours indicating the thickness of the boundary layer are given in Fig. 10. In the boundary layer, the velocity of the gas increases from zero on the wall surface to the maximum velocity of the flow. A turbulent boundary layer causes a larger momentum loss of the gas and leads to the rapid decay of the shock wave strength.

A larger boundary layer thickness was observed at a shock tube diameter of 3 mm compared to that in the 6 mm diameter shock tube. The boundary layer affects shock wave propagation with much more dissipation and viscous loss in shock tubes with smaller diameters. This makes the shock wave experience more attenuation. The contact surface at a shock tube diameter of 3 mm propagated faster compared to that at the shock tube diameter of 6 mm due to the thicker boundary layer. The thicker boundary layer makes a smaller velocity difference between the shock velocity and contact surface velocity. This results in a smaller distance L between the shock wave and contact surface in the shock tube of smaller scale.

5. Conclusions

Numerical simulations have been done to investigate the propagation of shock wave, contact surface and expansion waves. Effects of the scale and boundary layer development at different diaphragm pressure ratios and diameters in micro shock tube models have also been studied. Shock wave attenuation has been obtained at different shock tube diameters. Results show that the initial diaphragm pressure ratio influences the shock wave and contact surface propagation. As the diaphragm pressure ratio increases, the shock wave strength and contact surface propagation also increase. Reasonable deviations of shock wave, contact surface and expansion waves locations compared to theoretical results were observed, which results from the viscous effects, the friction between shock front and tube walls, and the boundary layer development in micro shock tubes.

Much stronger attenuation in the shock strength resulting from viscous boundary layer formation and effects of the scale happened in the shock tube of smaller scale. A thicker boundary layer that leads to much more loss in flow momentum and

shock wave propagation compared to the shock tube of larger scale was also observed in the smaller diameter shock tube. In addition, the thicker boundary layer developing in smaller scale shock tube obviously accelerates contact surface propagation. Present results also show that the scaling parameter S can indicate effects of the scale on shock wave propagation. Much more attenuation happened in the shock tube of 3 mm diameter with a smaller S value. In the future, PIV and Schlieren visualization measurement will be performed to validate the present theoretical conclusions and numerical results by qualitative analysis.

Acknowledgments

This work was supported by the National Research Foundation of Korea (NRF) grant funded by the Korea government (MEST) (2011-0017506).

Nomenclature

a : Speed of sound (m/s)
D : Shock tube diameter (mm)
L : Distance between shock wave and contact surface (mm)
M : Mach number
P : Static pressure (atm)
Pr : Pressure ratio
T : Total temperature (K)
t : Time (ms)
u : Velocity (m/s)
x : Axial coordinate
μ : Dynamic viscosity (Pa·s)
γ : Specific heat ratio
ρ : Density (kg/m^3)
δ : Boundary layer thickness (mm)

Subscripts

1 : Driven section
2 : Region between shock and contact surface
4 : Driver section

Reference

[1] R. E. Duff, Shock tube performance at initial low pressure, *Phys. Fluids*, 2 (1959) 207-216.
[2] D. E. Zeitoun, Y. Burtschell and I. A. Graur, Numerical simulation of shock wave propagation in micro channels using continuum and kinetic approaches, *Shock Waves*, 19 (2009) 307-316.
[3] D. E. Zeitoun and Y. Burtschell, Navier-Stokes computations in micro shock tubes, *Shock Waves*, 15 (2006) 241-246.
[4] M. Brouillete, Shock waves at microscales, *Shock Waves*, 13 (2003) 3-12.
[5] H. Mirels, Test time in low pressure shock tube, *Phys. Fluids*, 6 (1963) 1201-1214.
[6] B. Sturtevant and T. T. Okamura, Dependence of shock tube boundary layers on shock strength, *Phys. Fluids*, 12 (1969) 1723-1725.
[7] K. Tanaki, K. Inaba and M. Yamamoto, Numerical investigation on transition of shock induced boundary layer, *47th AIAA Aerospace Science Meeting including the New Horizons Forum and Aerospace Exposition*, 5-8 January 2009, Orlando, Florida (2009).
[8] D. Ngomo, A. Chaudhuri, A. Chinnayya and A. Hadjadj, Numerical study of shock propagation and attenuation in narrow tubes including friction and heat losses, *Computers & Fluids*, 39 (2010) 1711-1721.
[9] M. Sun, T. Ogawa and K. Takayama, Shock propagation in narrow channels, *Processing of 24th International Symposium on Shock Waves* (2001) 1321-1327.
[10] X. Hu, T. Aoki and N. Tokura, The feature of weak shock wave propagated in an overlong tunnel, *Open Journal of Fluid Dynamics*, 2 (2012) 285-289.
[11] K. A. Bhasakaran and P. Roth, The shock tube as wave reactor for kinetic studies and material systems, *Progress in Energy and Combustion Science*, 28 (2002) 151-192.
[12] K. R. Arun and H. D. Kim, Computational study of the unsteady flow characteristics of a micro shock tube, *JMST*, 27 (2012) 451-459.
[13] K. R. Arun and H. D Kim, Numerical visualization of the unsteady shock wave flow field in micro shock tube, *J. of the Korean Society of Visualization*, 10 (2012) 40-46.
[14] J. O. Park, G. W. Kim and H. D. Kim, Experimental study of the shock wave dynamics in micro shock tube, *J. of the Korean Society of Propulsion Engineers*, 17 (2014) 54-59.
[15] G. Mirshekari and M. Brouillette, One-dimensional model for microscale shock tube flow, *Shock Waves*, 19 (2009) 25-38.

Heuy Dong Kim received his B.S. degree and M.S. degrees in Mechanical Engineering from Kyungpook National University, Korea, in 1986 and 1988 respectively. He then received his Ph.D. from Kyushu University, Japan, in 1991. Currently, he is a professor at the Andong National University, Korea. His research interests include high-speed trains, ramjet and scramjet, shock tube and technology, shock wave dynamics, explosions and blast waves, flow measurement, aerodynamic noise, and supersonic wind tunnels.

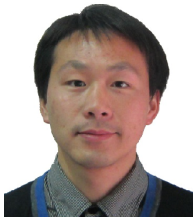

Guang Zhang received his B.S. degree in Mechanical Engineering from Three Gorges University, China, in 2012. Currently, he is pursuing his Master's in Andong National University. His research interests include micro shock tube and PIV measurement.